EFFECTS OF WATER ABSORPTION AND TEMPERATURE ON COMPRESSION AFTER IMPACT (CAI) STRENGTH OF CFRP LAMINATES

Yuichiro Aoki*, Ken Yamada and Takashi Ishikawa***
***Japan Aerospace Exploration Agency, Tokyo, Japan**
**** MAZDA Motor Corporation, Hiroshima, Japan**

Keywords: *water absorption, thermal environment, CAI strength, low velocity impact*

Abstract

This study investigated the combined effects of water absorption and thermal environment on compression after impact (CAI) characteristics of CFRP laminates. Specimens were immersed in 71℃ water for over 10,000 hours to quantify the ratio of water absorption in the CFRP laminates. Numerical simulation based on Fick's law was conducted to predict moisture diffusion using the measured orthotropic diffusion constants. Compression tests after drop-weight impact tests were carried out at various temperatures, i.e.,-54℃, 22℃, 82℃, 121℃, 149℃, 177℃. Delamination area and the number of transverse cracks of the wet specimen were smaller than those of dry specimens. Smaller delamination area of the wet specimens provides higher CAI strength than the dry specimens at mid-high temperature. The CAI strength of the wet CFRP decreased slightly at 149℃and significantly at 177℃ because the glass-transition temperature deteriorates seriously due to the water absorption.

1 Introduction

Carbon fiber reinforced plastic (CFRP) laminates are commonly used in a wide range of applications from sports equipment to aerospace structures to reduce the weight with high strength and stiffness. The structures made of composite laminates, however, are susceptible to impact damages such as delamination and transverse crack [1, 2]. These damages are barely visible from outside but cause a severe reduction of compressive performance of the structure. For this reason, the CAI strength is one of the most crucial factors to determine the design load in aircraft structure and material screening for new composite systems. Therefore, deep understanding in mechanics of CAI is indispensable to identify the dominant property of the test results and many works on CAI phenomenon have conducted by experiment and numerical analysis [3-9]. From these works, interesting characteristics of CAI behavior have been revealed, where the findings are divided into two phases: impact and compression. Impact-induced delamination is a crack which runs in the resin-rich area between layers of different fiber orientation and not between layers in the same orientation [8, 9]. The low-velocity impact test is sometimes replaced by static indentation tests since the damage configuration due to static indentation is similar to that of low-velocity impact [10-13]. The accumulation process of impact-induced damage is quite complex, and hence it is reasonable to investigate the damage problem under static loading instead of the complex impact response, and thereby avoiding such dynamic effects. For CAI strength, since the mode II fracture toughness, G_{IIC}, correlates with the impact resistance, increase of the G_{IIC} leads to obvious improvement of residual CAI strength [14, 15]. Analytical methods are also required to clarify the damage accumulation problems in composite laminates. Various numerical methods have been proposed to study the mechanism of damage accumulation in composite laminates. The virtual crack closure technique (VCCT) has been successfully used to study the stability of delamination propagation under the assumptions of initial delaminated area and self-similar delamination growth [16, 17]. In order to simulate progressive delaminations, interface models based on damage mechanics have been proposed and developed [18, 19]. A cohesive crack model based on the Dugdale-Barenblatt cohesive zone approach has also been introduced. The mechanical response of the cohesive model is determined by traction and energy dissipation in the vicinity of a crack tip. The cohesive model is convenient and attractive for simulating the delamination propagation in composite laminates since the fracture interface can be prescribed. Various cohesive elements have been developed and proposed for simulating the crack-like damage in composite materials [20-25].

On the other hand, composite aircraft structures are usually exposed to a range of hygrothermal conditions through their design service life, which causes degradation in material properties of CFRP laminates. The material degradation includes chemical changes of the matrix materials, debonding at fiber/matrix interface. Once water infuses into matrix or interface region of composite, the water would act as plasticizer, spacing the polymer chains apart, thus significantly lowering the glass transition temperature and internal stress built up during process is relieved. This phenomenon makes composites softer since the matrix becomes pliable due to the presence of the plasticizer. These changes affect the overall CFRP performances such as damage growth, strength and stiffness [26-30]. Most critical aspect of using CFRP in aircraft structures is performance of ‘hot-wet’ environments. Therefore, the identification of mechanism of degradation and levels of performance retention are critical for designers. Experimental and theoretical work on moisture absorption in composite materials is still an active research topic for a range of applications.

This study investigated the combined effects of water absorption and thermal environment on CAI characteristics of CFRP laminates. Numerical simulation using FEM code was also conducted to predict moisture diffusion based on the Fick’s law with measured orthotropic diffusion constants. Deterioration of the glass-transition temperature was evaluated by dynamic mechanical analyzer. Then, impact damage and residual CAI strength of water absorbed CFRP laminates were compared to dry conditioned CFRP laminates.

2 Preparation of specimens

The material system used in present study was T800H/3633, intermediate modulus, high tensile strength carbon fiber and 180 ℃ cure-type epoxy resin system, fabricated by TORAY Co., ltd. This material has a good high temperature resistant property and the interfaces between layers are toughened by distributed thermoplastic particles. A large amount of fundamental data for this material is obtained by our facility is available on internet website of JAXA-ACDB: http://www.jaxa-acdb.com.

The stacking sequence of the CAI specimen was $[45/0/-35/90]_{4s}$, with a nominal thickness of 4.5 mm. Specimens with dimensions of 150 × 100 mm were cut from the 3 batches of parent panel in reference to the SACMA SRM 2R-94 as well as ASTM 7136/D. The averaged fiber volume fraction was 57 %. In addition, unidirectional specimens with same material systems were prepared for measurement of orthotropic diffusion coefficients, where two directions of three material principal directions (i.e. fiber direction, in-plane transverse direction and out-of-plane direction) were sealed by aluminum foil shown as Fig. 1. All specimens were prepared at room temperature and visually inspected for any defects such as thickness variations which could lead to stress concentrations and affect the experimental data.

3 Experimental Procedures

3.1 Water absorption test

Accelerated water immersion tests were performed to quantify the ratio of water absorbed in the CFRP laminates. The pre-weighted dry specimens (dry specimen) were immersed in water bath with 71℃ distilled water for over 10,000 hours (i.e. 410 days) shown as Fig. 2. The weight gain of the immersed specimen (wet specimen) was periodically measured by electric weight scale. Water absorption M_t was calculated by following equation.

$$M_t = \frac{W_t - W_0}{W_0} \times 100 \qquad (1)$$

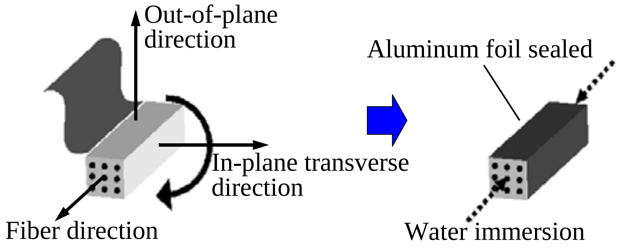

Fig.1 Preparation of unidirectional specimen for measurement of diffusivity in fiber direction

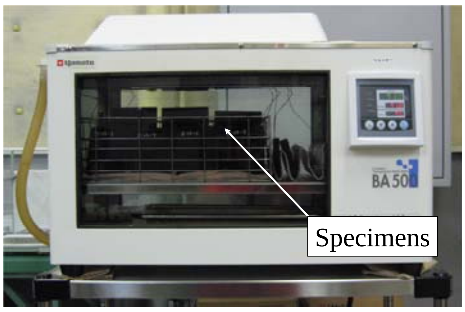

Fig.2 Overview of water absorption test

where, W_0 is weight of dry specimen and W_t is weight of wet specimen at time t.

Fick's diffusion law is employed to describe the diffusion coefficients in unidirectional orthotropic CFRP laminates. The governing equation of unidirectional diffusion described by Fick's law [31] is

$$D = \pi \left(\frac{h}{4M_s} \right)^2 \left(\frac{M_2 - M_1}{\sqrt{t_2} - \sqrt{t_1}} \right)^2 = \pi \left(\frac{h}{4M_s} \right)^2 k^2 \qquad (2)$$

where, h denotes thickness of the specimen in diffusion direction, Ms is saturation absorption and k means initial gradient of the water absorption curve. Since the diffusion in in-plane transverse direction and out-of-plane direction seems to be similar phenomenon, same coefficients are used for those directions in present study.

3.2 Impact test and damage inspection

Impact was given to the specimen by the drop-weight with a hemispherical impactor of 15.9 mm (5/8 inch) diameter were carried out at room temperature. The impact test machine is INSTRON 9250HV in which a rebound brake is attached to the test machine to prevent multiple impacts on the specimen by the impactor. The normalized impact energy is 3.3 J/mm which is a half energy level of the SACMA and ASTM standards. The specimen was clamped at four points by toggle rubbers as shown in the standards. Impact load, velocity and deflection of specimen were measured by an instrumented impactor and consider the behavior of impacted specimen.

After impact test, the size and shape of damages of the impacted specimen were inspected by the ultrasonic C-scan system (Krautkramer SDS5400R) with a 5 MHz transducer in pulsed-echo mode. The delamination area is defined by the projection area of the whole delamination obtained by C-scan image. After ultrasonic inspection, some of the specimens were cut into slices by diamond fine saw at their center and the through-the-thickness damage pattern was observed by a microscope.

3.3 Compression test

After impact tests, compression tests were carried out at various temperatures, i.e.,-54℃, 22℃, 82℃, 121℃, 149℃, 177℃. The number of specimen at each temperature is shown in Table 1. The compressive load was applied to the specimen under displacement control with a crosshead speed of 1.0 mm/min. CAI test fixture described in the SACMA standard is used (Fig. 3), which is designed to hold the specimen and out-of-plane displacement at side edges are simply supported by knife edge fixtures. The compressive load, displacement and strains are measured by KYOWA PCD-300 data logger with a sampling rate of 10 Hz during the test.

4 Results and Discussions

4.1 Water absorption

The average diffusivities are listed in Table 2. It is found that the diffusion in the fiber direction was much faster than that in the transverse direction, which implies water tends to penetrate along the

Table 1. Number of specimen

Specimen	Test temperature (℃)					
	-54	22	82	121	149	177
Dry	3	3	3	3	3	3
Wet	-	3	3	3	3	2

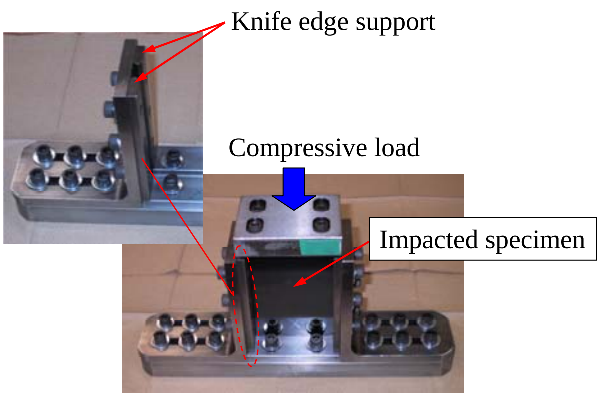

Fig.3 CAI test fixture

Table 2. Diffusivities of T800H/3633 UD laminates

	k (% $h^{1/2}$)	h (mm)	M_s (%)	D (mm^2/h)
Fiber direction	3.7 E-2	18.0	1.74	2.89 E-2
Transverse direction	3.6 E-2	3.9	1.73	1.17 E-3

fiber whereas carbon fiber dose not absorb water. Water absorption measurement and results of FEM analysis and theory are shown in Fig. 4. The water absorption calculated by Eq. 1 is plotted against square root of time. Saturation level of water absorption was 1.4% after the 10,000 hour water immersion test. Three-dimensional 8-node diffusion element with diffusivities in each direction listed in Table 1 was used. A commercially available finite element analysis code, ABAQUS Ver.6.6, was used for the present analysis. Normalized moisture concentration derived from Henry's law was applied to all surfaces of the finite element mesh. FEM prediction and theoretical curve based on Fick's law are also indicated. These curves agree well with experimental data. Water absorption in present CFRP laminates can be predicted by numerical method based on Fick's law. Figure 5 shows predicted water absorption process in present CAI specimen. The indicated value is saturation percentage at center of specimen which was normalized by saturation level of the absorption. The result shows that water diffused uniformly in every direction as a whole.

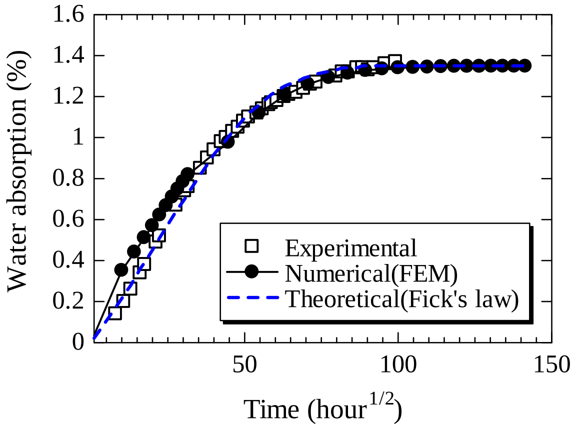

Fig.4 Water absorption in T800/3633 CFRP laminates immersed in water at 71℃.

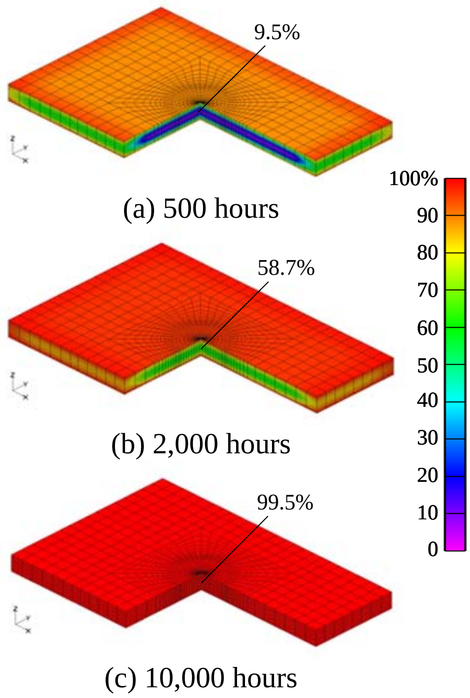

Fig. 5 Water absorption predicted by finite element analysis

4.2 Impact test results

Figure 6 shows the comparison of typical ultrasonic C-scan results after impact test for both specimens. From the images, it was found that average projected delamination area of the water absorbed CFRP was smaller than that of dry specimens. Figure 7 shows all the data of delamination area. Although the data shows some scatter, the delamination area of wet specimen is about 20% smaller than that of dry specimen. From cross-sectional observation shown as Fig. 8, however, the total number of delaminations through the thickness is larger than that of dry specimen while much more transverse cracks occurred in dry specimen.

These differences of impact damage characteristics were caused by the degradation of the resin and fiber/matrix interface. Once water infuses them, the water acts as plasticizer, spacing the polymer chains apart, thus CFRP laminates became softer. Therefore, the impact response was different between dry and wet specimens.

4.3 CAI test results

Figure 9 summarizes the CAI strengths of dry and water absorbed specimens at each temperature with reference information of the

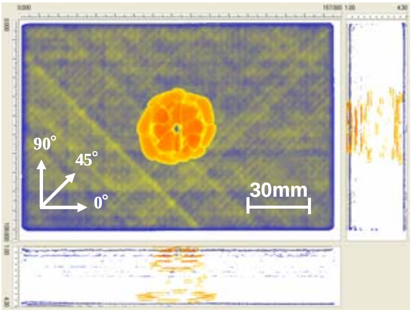

(a) Dry specimen

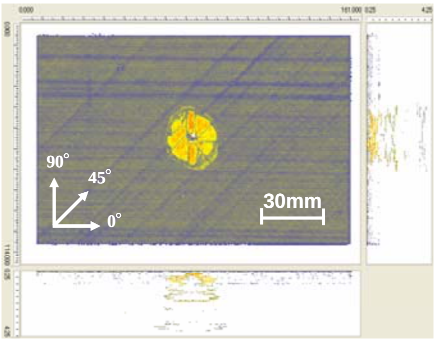

(b) Wet specimen

Fig.6 Comparison of the ultrasonic C-scanning images taken after impact test

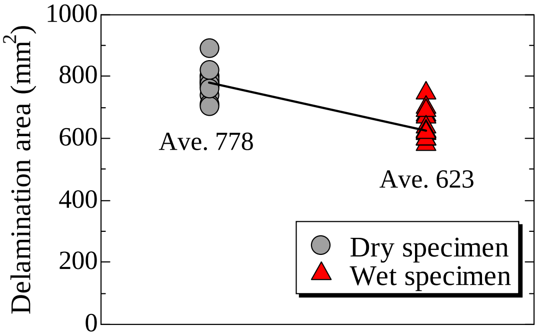

Fig. 7 Summary of delamination area after impact

interlaminar fracture toughness for mode I and mode II taken from JAXA-ACDB. Several important findings are shown in this figure, where two or three CAI data are included at each temperature point. The first point is that CAI strengths are well correlated with mode II fracture toughness at least from 22℃ to mid-high temperature of 121℃. The second finding is that CAI strengths of wet specimens are slightly higher than those of dry specimens from 22℃ to mid-high temperature of 121℃. This result implies that the projection size of delamination

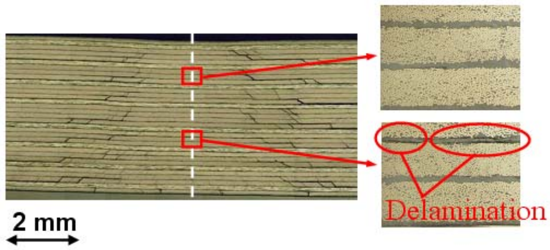

(a) Dry specimen

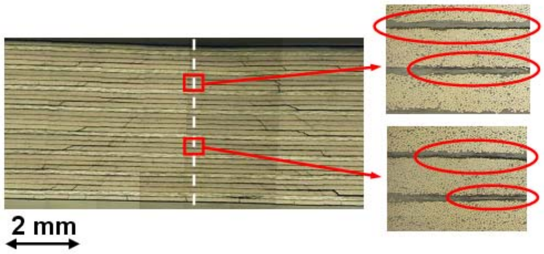

(b) Wet specimen

Fig.8 Cross sectional observations after impact test

mentioned above governs CAI strength. The third finding is a serious decrease of CAI strength in wet specimen at 177℃ that is most impressive result of present study. According to the measurement of the glass transition temperature (T_g) obtained by DMA (Dynamic Mechanical Analysis), it was decreased to 124℃ for the water absorbed specimen while the T_g of dry specimen is 174 ℃. Thus, the tested temperature of 177℃ for compression is quite high and then the compressive strength of water absorbed CFRP was almost lost. Ultrasonic C-scan results taken after compressive failure shown in Fig. 10 can

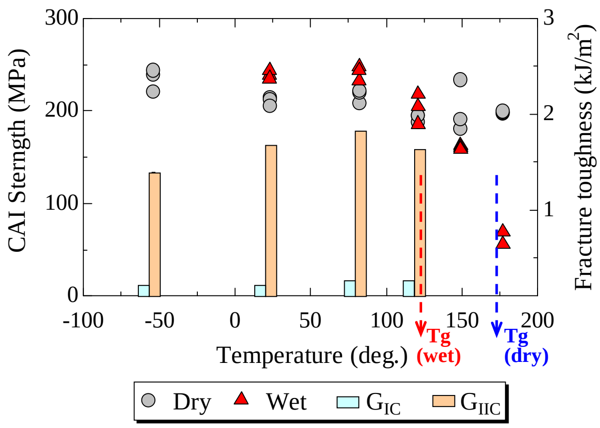

Fig.9 Relationships between CAI strength, interlaminar fracture toughness and temperature

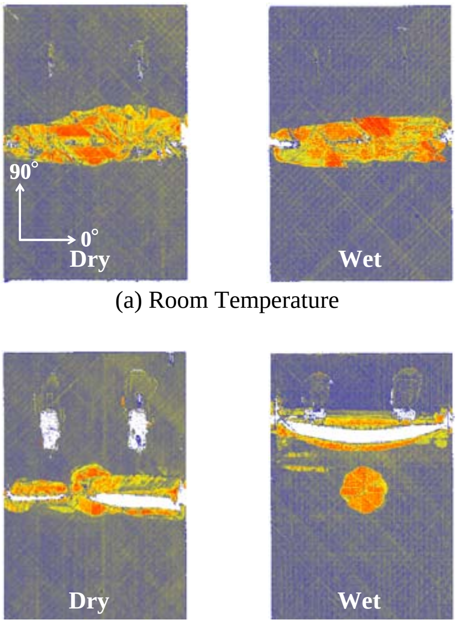

(a) Room Temperature

(b) 177 ℃

Fig.10 Ultrasonic C-scanning images taken after the compression tests

well explain the discussion above. In the case of 177℃ wet CAI test, impact induced delamination was not the trigger of the failure. Instead, buckling induced crippling type of failure was observed. These findings must be important and helpful information to understand the overall CAI behavior under hygrothermal environmental conditions.

4 Conclusions

The combined effects of water absorption and thermal environment on CAI characteristics of CFRP laminates are investigated in this study. The main conclusions are as follows.

- The moisture diffusion in the fiber direction was much faster (20 times) than that in the transverse direction.
- Numerical simulation based on Fick's law can predict the moisture diffusion using the measured orthotropic diffusion constants.
- Delamination area and the number of transverse cracks of the wet specimen are smaller than those of dry specimens since CFRP laminates is softened by water absorption.
- Glass transition temperature (T_g) of the CFRP laminates is significantly decreased by water absorption.
- The CAI strength of wet specimen are slightly higher than those of dry specimens from 22℃ to mid-high temperature of 121℃, which is well correlated with mode II fracture toughness.
- In the case of 177℃ wet CAI test, impact induced delamination is not the trigger of the failure but buckling induced crippling causes final failure.

References

[1] Richardson M. O. W. and Wisheart M. J., Review of low velocity impact properties of composite materials, *Composites A*, Vol. 27, pp.1123-1131, 1996.

[2] Abrate S., *Impact on composite structures*, Cambridge university press, Cambridge, 2005.

[3] Freitas M. de. and Reis L., Failure mechanisms on composite specimens subjected to compression after impact, *Composite Structures*, Vol. 42, pp 365-373, 1998.

[4] Hichen S. A. and Kemp R. M. J., The Effect of Stacking Sequence on Impact Damage in a Carbon Fiber/Epoxy Composite, *Composites*, Vol. 26, pp. 207-214, 1995.

[5] Shyr T.-W. and Pan Y.-H., Impact resistance and damage characteristics of composite laminates, *Composite Structures*, Vol. 62, No. 2, pp. 193-203, 2003.

[6] Ishikawa T., Sugimoto S., Matsushima M. and Hayashi Y., Some Experimental Findings in CAI Tests of CF/PEEK and Conventional CF/EPOXY Flat Plates, *Composites Science and Technology*, Vol. 55, pp. 349-362, 1995.

[7] Dost E. F., Ilcewicz L. B., and Avery W. B., The Effects of Stacking Sequence on Impact Damage Resistance and Residual Strength for Quasi-isotropic Laminates, *ASTM STP*, 1110, pp. 476-500, 1991.

[8] Wu H. Y. T. and Springer G. S., Measurements of Matrix Cracking and Delamination Caused by Impact on Composite Plates, *Journal of Composite Materials*, Vol. 22, No. 6, pp. 518-532, 1988.

[9] Cui W. and Wisnom M. R., A Combined Stress-Based and Fracture-Mechanics-Based Model for Predicting Delamination in Composites, *Composites*, Vol. 24, pp. 467-474, 1993.

[10] Sjöblom P. O., Hartness J. T. and Cordell T. M., On Low-velocity Impact Testing of Composite Materials, *Journal of Composite Materials*, Vol. 22, pp. 30-52, 1988.

[11] Wu E. and Shyu K., Response of Composite Laminates to Contact Loads and Relationship to Low-Velocity Impact, *Journal of Composite Materials*, Vol. 27, No. 15, pp. 1443-1464, 1993.

[12] Lee S. M. and Zahuta P., Instrumented Impact and Static Indentation of Composites, *Journal of Composite Materials*, Vol. 25, pp. 204-222, 1991.

[13] Kaczmarek H. and Maison S., Comparative ultrasonic analysis of damage in CFRP under static indentation and low-velocity impact, *Composites Science and Technology*, Vol. 51, No. 1, pp.11-26, 1994.

[14] Masters J. E., Correlation of Impact and Delamination Resistance in Interleafed Laminates, *Proceedings of ICCM VI & ECCM2*, London, 3:96, 1987.

[15] Chou, I, Namba, K., Correlation of Damage Resistance under Low Velocity Impact and Mode II Interlaminar Fracture Toughness in CFRP Laminates, *Advanced Composite Materials*, Vol. 8, No. 2, pp. 167-176, 1999.

[16] Razi H. and Kobayashi A. S., Delamination in cross-ply laminated composite subjected to low-velocity impact, *AIAA Journal*. Vol. 31, No. 8, pp. 1498-1502, 1993.

[17] Liu S. and Chang F. K., Matrix Cracking Effect on Delamination Growth in Composite Laminates Induced by a Spherical Indenter, *Journal of Composite Materials*, Vol. 28, 10, 940-977 (1994).

[18] Allix O. and Ladevèze P., Damage Analysis of Interlaminar Fracture Specimens, *Journal of Composite Materials*, Vol. 31, pp. 61-74, 1995.

[19] Mi Y., Crisfield M. A., Davies G. A. O. and Hellweg H. B., Progressive Delamination Using Interface Elements, *Journal of Composite Materials*, Vol. 32, pp. 1246-1273, 1998.

[20] Alfano C. and Crisfield M. A., Finite Element Interface Models for the Delamination Analysis of Laminated Composites: Mechanical and Computational Issues, *International Journal for Numerical Methods in Engineering*, Vol. 50, pp. 1701-1736, 2001.

[21] Borg R., Nilsson L. and Simonsson K., Modeling of Delamination using a Discredited Cohesive Zone and Damage Formulation, *Composites Science and Technology*, Vol. 62, pp. 1299-1314, 2002.

[22] Goyal V. K., Johnson E. R., Davila C. G. and Jaunky N., An Irreversible Constitutive Law for Modeling The Delamination Process using Interface Elements, *Proceedings of 43rd AIAA/ASME/ASCE/AHS/ASC Structures, Structural Dynamics, and Materials Conference*, Denver, Colorado, 2002.

[23] Aoki Y. and Suemasu H., Damage Analysis in Composite Laminates by using Interface Element, *Advanced Composite Materials*, Vol. 12, No. 1, pp. 13-22, 2003.

[24] Aoki Y., Suemasu H. and Ishikawa T., Damage propagation in CFRP Laminates subjected to low velocity impact and static indentation, *Advanced Composite Materials*, Vol. 16, No. 1, pp. 45-61, 2007.

[25] Ogi K., Kim H. S., Maruyama T. and Takao Y., Influence of Hygrothermal Conditions on the Damage Processes in Quasi-isotropic Carbon/Epoxy Laminates, *Composites Science and Technology*, Vol. 59, No. 16, pp. 2375-2382, 2000.

[26] Ogi K., Influence of thermal history on transverse cracking in a carbon fiber reinforced epoxy composite, *Advanced Composite Materials*, Vol. 11, No. 3, pp. 265-275, 2003.

[27] Tsenoglou C. J., Pavlidou S. and Papaspyrides C. D., Evaluation of interfacial relaxation due to water absorption in fiber–polymer composites, *Composites Science and Technology*, Vol.66, No. 15, pp. 2855-2864, 2006.

[28] Sala G., Composite degradation due to fluid absorption, *Composites Part B*, Vol. 31, No. 5, pp. 357-373, 2000.

[29] Abdel-Magid B., Ziaee S., Gass K. and Schneider M., The combined effects of load, moisture and temperature on the properties of E-glass/epoxy composites, *Composite Structures*, Vol. 71, No. 3-4, pp. 320-326, 2005.

[30] Shen C. H. and Springer G. S., Moisture Absorption and Desorption of Composite Materials, *Journal of Composite Materials*, Vol. 10, pp. 2-20, 1976.